Proc. Natl. Acad. Sci. USA
Vol. 89, pp. 9666–9670, October 1992
Neurobiology

Dendritic field size and morphology of midget and parasol ganglion cells of the human retina

(vision/primate/ON–OFF pathways/magnocellular pathway/parvocellular pathway)

DENNIS M. DACEY* AND MICHAEL R. PETERSEN

Departments of Biological Structure and Ophthalmology, University of Washington, Seattle, WA 98195

Communicated by John E. Dowling, June 29, 1992

ABSTRACT **The visual system of the macaque monkey has provided a useful model for understanding the neural basis of human vision, yet, there are few detailed comparisons of neural populations other than photoreceptors for the two species. Using intracellular staining in an *in vitro* preparation of the isolated and intact human retina, we have characterized the relationship of dendritic field size to retinal eccentricity for the two major ganglion cell classes, the midget and the parasol cells. We report three findings. (*i*) The difference in dendritic field diameter between the parasol and midget cells increases from a ratio of ≈3:1 in the retinal periphery to ≈10:1 at 3° eccentricity, suggesting that human midget cells may outnumber parasol cells by as much as 30:1 in the central retina. (*ii*) The dendritic fields of human ON-center parasol and midget cells are 30–50% larger in diameter than their OFF-center counterparts, suggesting a distinct asymmetry in the human ON–OFF visual pathways. (*iii*) The dendritic fields of parasol cells, but not midget cells, are larger in humans than in macaques. The difference increases from ≈20% in the retinal periphery to ≈90% at 5° eccentricity. This result predicts that the human parasol cells should show a lower resolving ability and an increased sensitivity to luminance contrast than their equivalents in the macaque.**

Neural pathways for the perception of color, form, and motion in the primate originate with at least two retinal ganglion cell classes, the midget and the parasol cells (1–3). Midget cells have small dendritic fields, reach a high density in the central retina, and make up the great majority of ganglion cells. Parasol cells have much larger dendritic fields and a lower spatial density. The midget and parasol cells project, respectively, to the parvocellular and magnocellular layers of the dorsal lateral geniculate nucleus (4). Neurons of the parvocellular pathway have small color-opponent-receptive fields and are necessary for the perception of color and fine detail (5, 6). Neurons of the magnocellular pathway have larger non-color-opponent-receptive fields and appear to compromise resolving ability to extend the range of vision to low levels of contrast and higher temporal resolution (5, 7). The magno- and parvocellular projecting cells are further divided into ON-center and OFF-center types that may subserve, respectively, the perception of light increment and decrement (8).

Similarities in visual psychophysical performance in human and macaque monkey (9, 10) suggest that the underlying neural properties of the parvocellular and magnocellular pathways are similar in the two species. Comparison of the physiological responses of macaque ganglion cells to visual stimuli with the psychophysically measured human responses to the same stimuli is consistent with this view, although some unexpected differences have been observed (11). Information on the physiological responses of human ganglion cells is limited to a single brief report on two cells (12), so that a direct comparison of human cell physiology to psychophysical measures has not been possible. At the anatomical level, human midget and parasol cells have been observed in Golgi preparations (13–15), but a description of human retinal ganglion cell morphology, obtained with techniques that would permit a detailed comparison with the macaque, has also not been technically possible.

In this report we show that the morphology of human retinal ganglion cells can be demonstrated by intracellular injection of either horseradish peroxidase (HRP) or the biotin compound Neurobiotin in an *in vitro* preparation of intact retina. When the human retina was obtained within 2 h of death, it could be maintained easily *in vitro* for many hours. Intracellularly stained neurons showed excellent preservation of morphology that was of the same quality as in similar preparations of *in vitro* macaque retina (3, 16). We present three findings about the midget and parasol cell populations that suggest quantitative differences between human and macaque in properties of the parasol–magnocellular system and a distinct asymmetry in the ON–OFF pathways in the human.

METHODS

Nomenclature. The midget and parasol ganglion cells have also been referred to, respectively, as A and B cells, Pbeta and Palpha cells, and P (parvocellular projecting) and M (magnocellular projecting) cells. We have chosen to use the parasol and midget terminology (*i*) because there is a precedent for this in the human retina (14) and (*ii*) because there is growing evidence in the macaque that parvocellular and magnocellular projecting cells include cell types beyond the midget and parasol cells (11). Thus the P and M terminology refers to some number of ganglion cell types, the most common of which are the midget and parasol cells, respectively. A more detailed discussion of these issues can be found in Watanabe and Rodieck (3) and Peichl (17).

***In Vitro*-Isolated Retina.** The *in vitro* retinal whole-mount preparation and intracellular injection technique were developed for the macaque and other mammalian retinas (3, 18, 19). Human eyes (n = 44; age range, 16–82 years) were obtained from eye-bank donors from 90 to 120 min after death. The vitreous was removed and the retina was dissected free of the sclera and choroid in a continuously oxygenated culture medium (Ames; Sigma). Isolated retinas underwent a 1- to 2-h recovery period and then were placed flat with the photoreceptor side down in a superfusion chamber on the stage of a light microscope. Ganglion cells were stained with the fluorescent vital dye acridine orange and observed under blue episcopic illumination. Retinas were

The publication costs of this article were defrayed in part by page charge payment. This article must therefore be hereby marked "*advertisement*" in accordance with 18 U.S.C. §1734 solely to indicate this fact.

Abbreviation: HRP, horseradish peroxidase.

*To whom reprint requests should be addressed.

typically maintained *in vitro* for more than 10 h with no apparent deterioration in morphology.

Intracellular Injection. Intracellular injections were made under direct microscopic control with beveled microcapillary electrodes. Electrodes were filled with a solution of either rhodamine-conjugated HRP [≈4% (wt/vol); Sigma] or Neurobiotin [≈4% (wt/vol); Vector Laboratories] and Lucifer yellow [≈2% (wt/vol); Aldrich] in 20 mM lithium hydroxide and beveled to a resistance of ≈40 MΩ. Lucifer yellow fluorescence in the electrode and the acridine orange fluorescence of the ganglion cells were observed with the same excitation filter (410–490 nm; barrier filter, 515 nm), permitting direct observation of the microcapillary tip as it penetrated a cell. Ganglion cells were filled with HRP or Neurobiotin and the HRP reaction product was detected after fixation of the retina as described (16, 20).

Comparison with Macaque Monkey. To compare the sizes of the macaque and human midget and parasol cells, distance from the fovea in mm was converted to degrees of visual angle. In the human the nonlinear conversion of Drasdo and Fowler (21) was used. In this schematic eye, the distance to angle conversion is 275 μm/degree in the fovea and decreases to ≈135 μm/degree at 90° eccentricity. The nonlinear relationship between retinal distance and visual angle (figure 2 in ref. 21) is well fit by the second-order polynomial equation $y = 0.1 + 3.4x + 0.035x^2$ ($R = 1.0$), where y is the eccentricity in degrees and x is the eccentricity in mm. For the smaller eye of the macaque, the distance to angle conversion reported by Perry and Cowey (22) was used. These authors found a foveal conversion of 223 μm/degree that declined to ≈170 μm/degree in the far retinal periphery. The nonlinear relationship between retinal distance and visual angle (figure 4 in ref. 22) is well fit by the second-order polynomial equation $y = 0.1 + 4.21x + 0.038x^2$ ($R = 1.0$).

Conversion to angular eccentricity in the central retina is further complicated by the lateral displacement of ganglion cells from the inner segments of the photoreceptors from which they receive input. Therefore, ganglion cell eccentricity was converted to inner segment eccentricity for all cells within 3 mm of the fovea. For the monkey, the data in figure 17b of ref. 23, based on direct measurements of photoreceptor axons (Henle fibers), were used to calculate inner segment eccentricity. These data were best fit by the following equation: $y = -0.23 + 0.87x + 0.086x^2$ ($R = 1.0$), where y is the inner segment eccentricity in mm and x is the ganglion cell eccentricity in mm. In the human retina there is evidence that Henle fibers are longer than in the macaque (24). A second equation was, therefore, generated to correct for ganglion cell displacement in human also based on direct measurements of Henle fiber lengths (C. Curcio, personal communication). For the human retina, $y = -0.020 + 0.46x + 0.20x^2$ ($R = 1.0$), where y is the inner segment eccentricity in mm and x is the ganglion cell eccentricity in mm.

RESULTS

Human Parasol and Midget Dendritic Field Size. The dendritic field size, retinal location, and detailed morphology of ≈1300 HRP-filled human retinal ganglion cells were studied. Of these, 277 were easily identified as parasol cells and 365 were identified as midget cells by their small densely branching narrowly stratified dendritic trees (Fig. 1) and their clear similarity to macaque midget and parasol cells (3). By contrast, all other narrowly monostratified ganglion cell types had much larger and more sparsely branching dendritic fields than the midget and parasol cells. Other cell types that fell within the midget–parasol dendritic field size range could also be distinguished by their distinctly bistratified or diffusely branching dendritic trees (25).

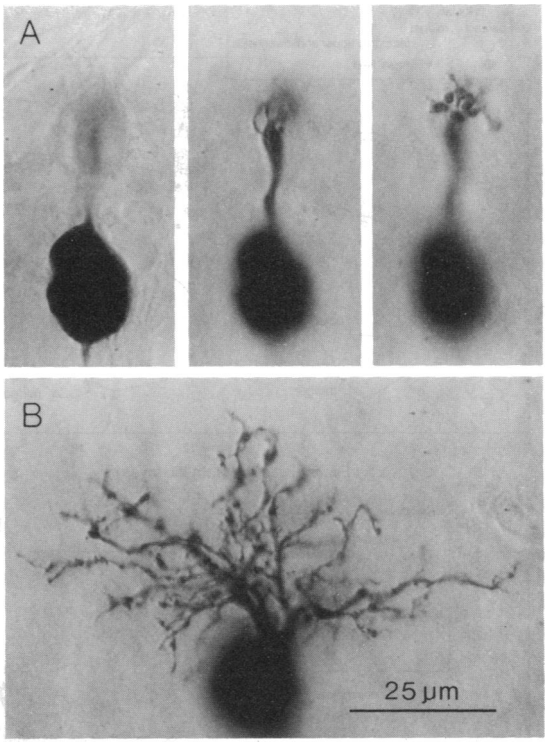

FIG. 1. (*A*) Photomicrographs of an intracellular Neurobiotin-filled midget cell in the temporal retina, 500 μm from the foveal center in a retinal whole-mount preparation. The plane of focus shifts from the cell body (*Left*) to the primary and secondary dendrites (*Center*) and then to the small cluster of dendritic terminals (*Right*). (*B*) Intracellular Neurobiotin-filled parasol cell in the temporal retina, 600 μm from the foveal center in a retinal whole-mount preparation. The cell body is slightly out of the plane of focus. (Scale bar refers to *A* and *B*.)

When dendritic field diameter was plotted as a function of distance from the fovea, the human midget and parasol cells formed two distinct clusters that gradually decreased in size with decreasing distance from the fovea (Fig. 2*A*). Cells lying in the nasal retinal quadrant were smaller than those in the temporal, upper, and lower quadrants, consistent with previous results in the macaque using the same intracellular injection technique (3).

In addition to their smaller size, the midget cells also showed a greater decrease in dendritic field size with decreasing eccentricity than the parasol cells. The result was that the difference in size between the midget and parasol cells increased toward the fovea (Fig. 2*B*). Thus the ratio of parasol to midget cell dendritic field diameter increased from ≈3:1 at 50° retinal eccentricity to ≈10:1 at 3° (1.4 mm) from the fovea.

Comparison with Macaque. The relationship of dendritic field size to retinal eccentricity for human midget and parasol cells was compared to that for the macaque retina (3). On average parasol cells were larger in humans than in macaques (Fig. 3*A*). The difference in size was small in the retinal periphery and gradually became larger with decreasing eccentricity. At 40°, human parasol cells were ≈20% larger in diameter and at 5° they were ≈90% larger than macaque parasol cells. In contrast human and macaque midget cells were similar in size at all retinal eccentricities (Fig. 3*B*).

ON–OFF Asymmetry. Parasol and midget cells can be divided into types whose dendritic trees stratify in either the inner or outer portions of the inner plexiform layer and are believed to correspond respectively to ON- and OFF-center cells (3). Human parasol and midget cells that branched in the inner third (presumed ON-center cells) or outer third (pre-

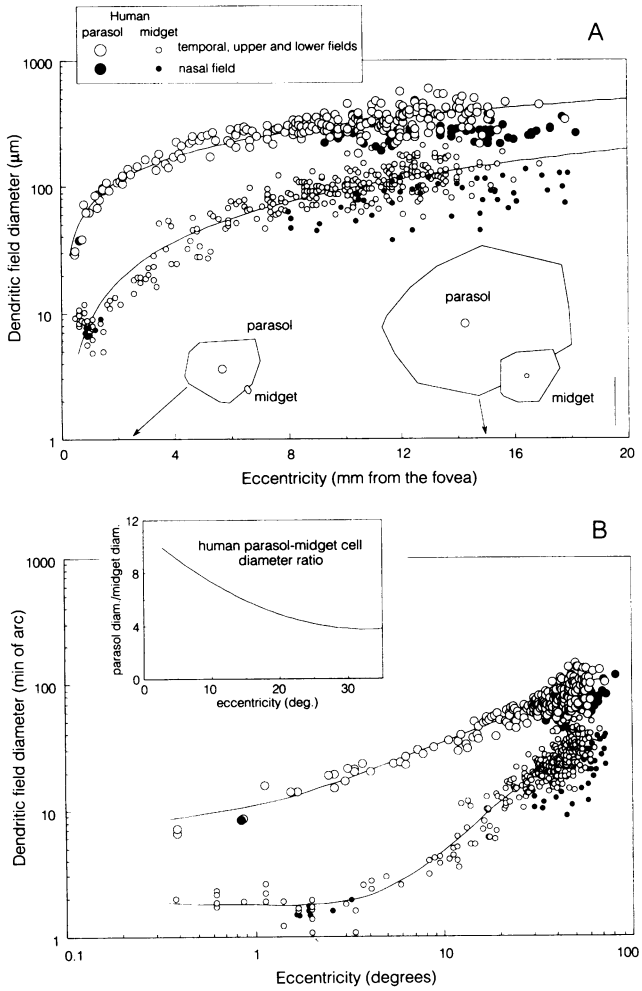

FIG. 2. Relationship of dendritic field size to retinal eccentricity for human midget and parasol ganglion cells. (*A*) The midget and parasol cells form two distinct clusters. Cells of the nasal quadrant (solid symbols) were smaller than cells of the temporal, upper, and lower quadrants (open symbols). The curves fit to the two sets of data points are logarithmic functions and apply to the cells of the temporal, upper, and lower quadrants only; for the midget cells, $y = 8.64 \times x^{1.04}$ ($R = 0.94$), and for the parasol cells, $y = 70.2 \times x^{0.65}$ ($R = 0.92$). The polygon insets are tracings around the dendritic trees of midget and parasol cells and indicate relative differences in dendritic field size at 2.5 and 15 mm eccentricity. (Vertical scale bar in the lower right = 100 μm.) (*B*) Scatter plot for the data in *A* shown on log-log coordinates with dendritic field size expressed in minutes of arc and eccentricity expressed in degrees of visual angle. (*Inset*) The ratio of parasol to midget dendritic field diameter is plotted. The curves fit to the data are fourth-order polynomial functions. For the midget cells, $R = 0.86$; for the parasol cells, $R = 0.87$.

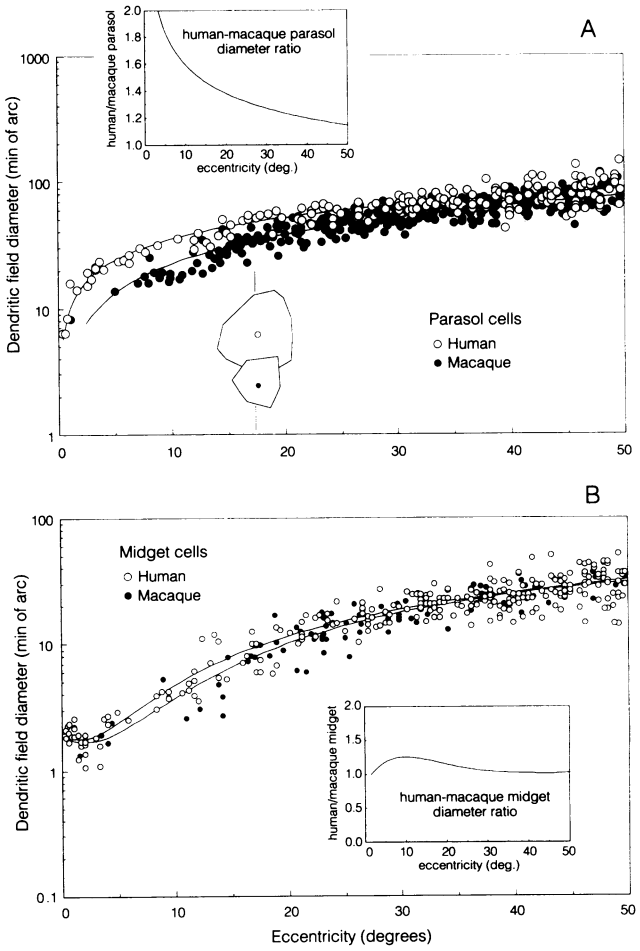

FIG. 3. Human midget and parasol data from the temporal, upper, and lower retinal quadrants shown in Fig. 2 are compared to published data from the macaque retina (3). (*A*) Dendritic field diameters of human parasol cells are larger than macaque parasol cells. (*Inset*) Ratio of human to macaque parasol dendritic field size from 5 to 50° eccentricity. The difference between the slopes of the two parasol curves was highly significant (t value = 9.59; $P < 0.0001$). The polygon insets were traced around a single human (upper polygon) and macaque (lower polygon) parasol dendritic tree at 17° eccentricity. (*B*) The human and macaque midget cell clusters were similar in size at all retinal eccentricities. (*Inset*) Ratio of human to macaque midget dendritic field size.

sumed OFF-center cells) of the inner plexiform layer could be distinguished and their distinct levels of stratification were verified in ON–OFF cell pairs (Fig. 4) or in radial histological sections (data not shown). For both midget and parasol cell pairs, ON-center cells consistently showed 30–50% larger dendritic field diameters than their OFF-center counterparts (Fig. 5). This difference was independent of dendritic field size over the eccentricity range (2–15 mm from the fovea) that ON–OFF cell pairs were sampled.

DISCUSSION

Midget and Parasol Cells: Two Ganglion Cell Classes. The midget and parasol ganglion cells of the human retina can be distinguished at all retinal eccentricities by their distinctive dendritic morphology. When plotted as a function of retinal eccentricity, the dendritic field diameters of the midget and parasol cells also occupy two distinct clusters, reinforcing the conclusion that these cells include only two distinct cell classes. This result is consistent with a previous study of human Golgi-impregnated cells (14) and with intracellular filling (3) and retrograde labeling (2) of macaque retinal ganglion cells. Surprisingly, all of these results stand in sharp contrast to a recent study of Golgi-impregnated cells in the human retina by Kolb *et al.* (15) that identified two nonoverlapping size groups in the midget cluster: cells with extremely small dendritic fields (5–15 μm in diameter, termed P1 cells) and those with larger fields (10–60 μm, termed P2 cells). However, many of the dendritic field size measurements of the midget cells given in our data fall squarely in between the P1 and P2 size groups. Our midget sample, therefore, shows only a single cluster with a normally distributed scatter at each eccentricity and no indication of the extreme bimodal distribution illustrated by Kolb *et al.* (15).

Relative Spatial Density of Midget and Parasol Cells. In the macaque retina, there is evidence that the midget and parasol cells make up, respectively, ≈80% and 10% of the total

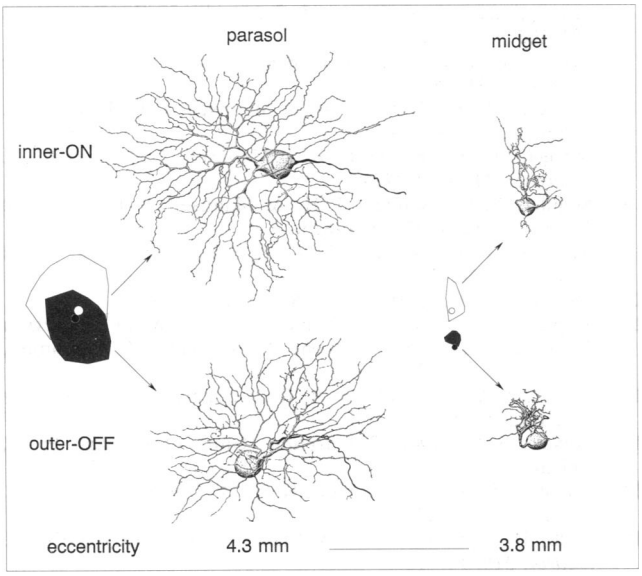

FIG. 4. Detailed dendritic morphology of inner (presumed ON-center) and outer (presumed OFF-center) branching pairs of parasol (to the left) and midget (to the right) cells in the human retina. The relative positions of each pair of cells in the retinal wholemount are shown by the polygons and their retinal eccentricity is shown at the bottom of the figure. Each polygon marks the extremities of the dendritic tree and the small circle denotes the cell body. ON-center cells (open) are larger than their OFF-center (shaded) counterparts for both midget and parasol cell types. (Bar = 100 μm.)

ganglion cell population and that this ratio of midget to parasol cells does not change from central to peripheral retina (2, 26). However, there is also conflicting evidence [for review, see Schein and de Monasterio (27)] that the ratio of magnocellular- to parvocellular-projecting neurons changes dramatically as a function of eccentricity in the visual field. In the human retina, we have shown that the ratio of parasol to midget dendritic field diameter also changes dramatically as a function of eccentricity (Fig. 2*B*), and this result has implications for understanding the spatial organization of these two cell populations. The ratio of parasol to midget field size increases toward the fovea, suggesting two possibilities. (*i*) Parasol cell density increases more slowly approaching the central retina than does midget cell density, and dendritic overlap (dendritic field area × cell density) remains constant. (*ii*) The densities of the two populations increase at the same rate, but dendritic overlap for parasol cells is much greater in central than in peripheral retina.

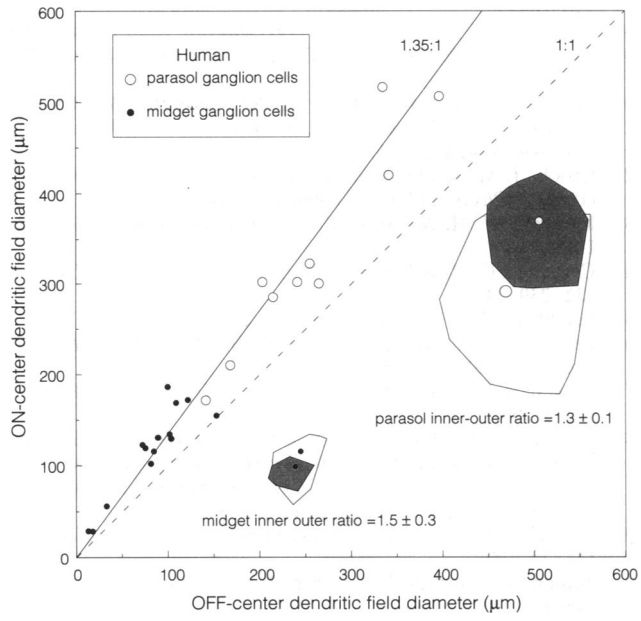

FIG. 5. Ratio of inner branching (presumed ON-center) to outer branching (presumed OFF-center) dendritic field diameter is plotted for the midget (small symbols) and parasol (large symbols) cells. The dotted line marks the predicted unity ratio for the inner and outer types. ON-center cells were larger than OFF-center cells for both midget [1.5 ± 0.3 (mean ± SD; n = 14] and parasol cell pairs [1.3 ± 0.1 (mean ± SD; n = 10]. The solid line shows a ratio of 1.35:1 that was fit by eye through both the midget and parasol data. The polygon pair insets show tracings around the dendritic field of an inner (open) or outer (shaded) ganglion cell. The position of the soma for each cell is marked by the small circle within each polygon.

A major reason for favoring the first possibility is that the maintenance of a constant dendritic field overlap appears to be a characteristic feature of ganglion cell mosaics (28). What variation in overlap would we expect if the second alternative was correct? If the human midget to parasol density ratio is a constant 8:1, as suggested in the macaque, then, given the dendritic field size measurements shown here, the ON and OFF human parasol cells would each need to attain an unprecedented overlap of 12 in the central retina compared to 1 for the midget cells. Such large changes in dendritic field coverage as a function of eccentricity have not been observed for any vertebrate ganglion cell population and would require an extremely dense packing of parasol cell bodies that has not been observed. If the dendritic field overlap for the human midget and parasol cells is constant, what would the relative densities of the two populations be? In the macaque retina dendritic field overlap for the parasol cells is 3.4 and has been estimated for the midget cells to be 1–2 (2, 28). We have found that the human parasol/midget dendritic field diameter ratio ranges from ≈3:1 to ≈10:1, giving an areal ratio of 9:1 to 100:1. Dividing these dendritic field areas by the coverage values gives a midget/parasol cell density ratio that ranges from ≈3:1 in the retinal periphery to ≈30:1 at 3° (1.4 mm) eccentricity. In the dorsal lateral geniculate nucleus, cell density measurements suggest a similar change in the relative densities of parvocellular and magnocellular neurons from 4:1 in the far periphery to close to 40:1 in the foveal representation (29). Comparison of geniculate cell densities with striate cortex (V1) magnification has led to the hypothesis that V1 magnification is proportional to, and thus based on, parvocellular cell density (27). The present results are consistent with the hypothesis that the density gradient of midget ganglion cells alone can account for the V1 magnification.

The possibility that the midget cells greatly outnumber the parasol cells in the central retina has significance for understanding the role played by these two cell populations in visual sensitivity. There is compelling psychophysical evidence that the midget–parvocellular pathway is critical for the perception of fine detail. Midget cells establish a sampling mosaic of appropriate density to account for the highest visual acuity and the decline of acuity with distance from the fovea (30, 31), and lesions of the parvocellular pathway drastically affect the perception of fine detail (5, 6). However, the resolving power of individual midget cells studied electrophysiologically is, somewhat paradoxically, no better than that of parasol cells at the same eccentricity, probably due to a lower contrast sensitivity (32). It has been suggested that the sensitivity of the midget cells as a population could be increased to the level of the parasol cells by summing the signals from a number of midget cells (33), but the midget/parasol ratio reported previously in the macaque is not great enough to achieve this result (11). However, as discussed above, a midget/parasol ratio of ≈30:1 may be attained in the

human parafoveal retina, suggesting the possibility of a relative increase in midget sensitivity by summation.

Magnocellular Pathway. The difference in parasol dendritic field size (Fig. 3*A*) could underlie differences between human and macaque visual capabilities thought to depend on the magnocellular pathway. The larger size of the human parasol cells, especially in the central retina, predicts a lower spatial density (if dendritic overlap is comparable) and correspondingly lower resolving ability for the cell mosaic. It has been suggested that the increased sensitivity of the magnocellular cells to luminance contrast is one consequence of their larger receptive fields. If this is true, then under stimulus conditions that tend to selectively excite the magnocellular pathway (i.e., low contrast, low spatial frequency, and high temporal frequency), humans might show greater visual sensitivity but poorer acuity than macaque. In support of this idea, macaque visual acuity under scotopic conditions is superior to human acuity (34), whereas human vision has the edge in measures of both spatial contrast sensitivity and temporal vision (9, 10).

ON–OFF Asymmetry. We have shown that for pairs of inner (presumed ON-center) and outer (presumed OFF-center) branching midget and parasol cells the ON-center cells had 30–50% larger dendritic field diameters than their OFF-center counterparts. A similar difference in presumed ON- and OFF-center field size has been observed previously for the parasol cell equivalent in the rat retina (35), but in other mammalian retinas, including the macaque, dendritic-field size differences between ON- and OFF-center ganglion cells have not been observed (36). The ON–OFF dendritic field size asymmetry in the human retina would predict that OFF-center cells have smaller receptive fields, form a mosaic of higher cell density, and thus have greater resolving power than ON-center cells. Psychophysical tests designed to selectively stimulate either the ON or the OFF visual pathway also suggest asymmetries in the size or sensitivity of the visual receptive fields that form these two channels (37–39). A recent study of human visual-evoked potentials generated by positive and negative contrast stimuli that gave rise to the perception of brightness and darkness concluded that the response to stimulation of the OFF pathway showed finer spatial tuning than the ON-pathway response (40). Whether a similar ON–OFF functional asymmetry is present in macaque vision has not, to our knowledge, been studied.

We thank especially Kim Allen and the staff of the Lions Eye Bank for the timely retrieval of donor eyes for this research. We also thank Sarah Brace and Kim Zigmond for technical assistance. Christine Curcio, Margy Koontz, Kate Mulligan, Tom Reh, Helen Sherk, Paul Martin, Thom Hughes, and Heinz Wässle offered helpful comments on various drafts of this paper. This work was supported by National Institutes of Health Grants EY 07031 (M.R.P.) and EY 06678 (to D.M.D.).

1. Leventhal, A. G., Rodieck, R. W. & Dreher, B. (1981) *Science* **213**, 1139–1142.
2. Perry, V. H., Oehler, R. & Cowey, A. (1984) *Neuroscience* **12**, 1101–1123.
3. Watanabe, M. & Rodieck, R. W. (1989) *J. Comp. Neurol.* **289**, 434–454.
4. Lennie, P., Trevarthen, C., Van Essen, D. & Wässle, H. (1990) in *Visual Perception: The Neurophysiological Foundations*, eds. Spillmann, L. & Werner, J. S. (Academic, San Diego), pp. 103–128.
5. Schiller, P., Logothetis, N. K. & Charles, E. R. (1990) *Nature (London)* **343**, 68–70.
6. Merigan, W. H., Katz, L. M. & Maunsell, J. H. R. (1991) *J. Neurosci.* **11**, 994–1001.
7. Merigan, W. H., Byrne, C. E. & Maunsell, J. H. R. (1991) *J. Neurosci.* **11**, 3422–3429.
8. Schiller, P. H., Sandell, J. H. & Maunsell, J. H. R. (1986) *Nature (London)* **322**, 824–825.
9. deValois, R. L., Morgan, H. C. & Snodderly, D. M. (1974) *Vision Res.* **14**, 75–82.
10. Merigan, W. H. (1980) *Vision Res.* **20**, 953–959.
11. Kaplan, E., Lee, B. B. & Shapley, R. M. (1990) in *Progress in Retinal Research*, eds. Osborne, N. & Chader, J. (Pergamon, New York), pp. 273–336.
12. Weinstein, G. W., Hobson, R. R. & Baker, F. (1971) *Science* **171**, 1021–1022.
13. Polyak, S. L. (1941) *The Retina* (Univ. of Chicago Press, Chicago).
14. Rodieck, R. W., Binmoeller, K. F. & Dineen, J. (1985) *J. Comp. Neurol.* **233**, 115–132.
15. Kolb, H., Linberg, K. A. & Fisher, S. K. (1992) *J. Comp. Neurol.* **318**, 147–187.
16. Dacey, D. M. (1989) *J. Comp. Neurol.* **284**, 275–293.
17. Peichl, L. (1991) *Visual Neurosci.* **7**, 155–169.
18. Vaney, D. I. (1986) *Science* **233**, 444–446.
19. Dacey, D. M. (1988) *Science* **240**, 1196–1198.
20. Dacey, D. M. & Brace, S. (1992) *Vis. Neurosci.* **9**, 279–290.
21. Drasdo, N. & Fowler, C. W. (1974) *Br. J. Ophthalmol.* **58**, 709–714.
22. Perry, V. H. & Cowey, A. (1985) *Vision Res.* **25**, 1795–1810.
23. Schein, S. J. (1988) *J. Comp. Neurol.* **269**, 479–505.
24. Curcio, C. A. & Allen, K. A. (1990) *J. Comp. Neurol.* **300**, 5–25.
25. Dacey, D. M., Petersen, M. & Allen, K. (1991) *Invest. Ophthalmol. Visual Sci.* **32**, 1130 (abstr.).
26. Silveira, L. C. L. & Perry, V. H. (1991) *Neuroscience* **40**, 217–237.
27. Schein, S. J. & de Monasterio, F. M. (1987) *J. Neurosci.* **7**, 996–1009.
28. Wässle, H. & Boycott, B. B. (1991) *Physiol. Rev.* **71**, 447–480.
29. Connolly, M. & Van Essen, D. (1984) *J. Comp. Neurol.* **226**, 544–564.
30. Merigan, W. H. & Katz, L. M. (1990) *Vision Res.* **30**, 985–991.
31. Thibos, L. N., Cheney, F. E. & Walsh, D. J. (1987) *J. Opt. Soc. Am. A* **4**, 1524–1529.
32. Crook, J. M., Lange-Malecki, B., Lee, B. B. & Valberg, A. (1988) *J. Physiol. (London)* **396**, 205–224.
33. Merigan, W. H. & Eskin, T. A. (1986) *Vision Res.* **26**, 1751–1761.
34. Cavonius, C. R. & Robbins, D. O. (1973) *J. Physiol. (London)* **232**, 239–246.
35. Peichl, L. (1989) *J. Comp. Neurol.* **286**, 120–139.
36. Peichl, L., Ott, H. & Boycott, B. B. (1987) *Proc. R. Soc. London B* **231**, 169–197.
37. Bowen, R. W., Pokorny, J. & Smith, V. (1989) *Vision Res.* **29**, 1501–1509.
38. Fiorentini, A., Baumgartner, G., Magnussen, S., Schiller, P. H. & Thomas, J. P. (1990) in *Visual Perception: The Neurophysiological Foundations*, eds. Spillmann, L. & Werner, J. S. (Academic, San Diego), pp. 129–161.
39. Tyler, C. W., Chan, H. & Liu, L. (1992) *Ophthal. Physiol. Opt.* **12**, 233–240.
40. Zemon, V., Gordon, J. & Welch, J. (1988) *Visual Neurosci.* **1**, 145–150.